

This is a non-peer-reviewed preprint submitted to EarthArXiv.

This manuscript has yet to be formally accepted for publication.
Subsequent versions of this manuscript may have slightly different
content.

Paleoecology indicates wave climate as key factor in coral reef development

Patrick Boyden^{1,2*†}, Donghao Li¹, Sonia Bejarano³, Benjamin Mueller^{2,4}, Christian Wild², Eric Mijts⁵, Giovanni Scicchitano^{6,7}, Giovanni Scardino^{6,7}, Denovan Chauveau⁸, Ute Merkel¹, Yusuf C. El-Khaled^{2,9}, Paolo Stocchi¹⁰, Mark Vermeij^{4,11}, Alessio Rovere^{1,12*†}

¹ *MARUM - Center for Marine Environmental Sciences, University of Bremen, Leobener Str. 8, Bremen, 28359, Germany.

² Faculty of Biology and Chemistry, University of Bremen, Bibliothek Str. 1, Bremen, 28359, Germany.

³ Leibniz Centre for Tropical Marine Research, Fahrenheit str. 6, Bremen, 28359, Germany.

⁴ CARMABI Foundation, Piscaderabaai, Willemstad, Curaçao.

⁵ University of Aruba, J. Irausquin Plein 4, Oranjestad, Aruba.

⁶ Department of Earth and Geo-Environmental Sciences, University of Bari Aldo Moro, Via Orabona 4, Bari, 70125, Italy.

⁷ Interdepartmental Research Center for Coastal Dynamics, University of Bari Aldo Moro, Via Orabona 4, Bari, 70125, Italy.

⁸ Geo-Ocean, UMR 6538, CNRS, Ifremer, Université de Bretagne Occidentale, Plouzané, F-29280, France.

⁹ King Abdullah University of Science and Technology, Street, Thuwal, 23955-6900, Kingdom of Saudi Arabia.

¹⁰ Dipartimento di Scienze Puree Applicate, University Of Urbino "Carlo Bo", Via Santa Chiara 27, Urbino, 61029, Italy.

¹¹ Department of Freshwater and Marine Ecology, Institute for Biodiversity and Ecosystem Dynamics, University of Amsterdam, P.O. Box 94240, Amsterdam, 1090 GE, The Netherlands.

¹²* Department for Environmental Sciences, Informatics and Statistics, Ca' Foscari University of Venice, Via Torino 155, Venice, 30172, Italy.

*Correspondence to: Patrick Boyden (ptboyden@gmail.com) and Alessio Rovere (alessio.rovere@unive.it)

Abstract. The Last Interglacial (~125,000 years ago) experienced global temperatures warmer than today, making it a natural analog for future climate scenarios. Contemporary coral reefs preserve ecological signals that offer valuable insights into past climate dynamics. Here, we examine the fossil reefs of Aruba, Bonaire, and Curaçao to reconstruct wind and wave conditions during this period. While modern reefs across all three islands are confined predominantly to leeward coasts, paleo reefs flourished on both windward and leeward coasts during the Last Interglacial—raising questions as to what mechanisms underlie the spatial asymmetry in reef development through time. Using quantitative analyses of hard coral cover and changes in coral community composition across the Last Interglacial, we document a transition from a well-developed reef dominated by large colonies of *Orbicella* spp. and *Acropora palmata* to a less structurally complex system characterized by smaller *Orbicella* spp. and *Diploria* spp. colonies, mirroring a ~20% reduction in hard coral cover by the end of the Last Interglacial. Despite this decline, coral cover remained substantial and did not resemble the Sargassum-dominated nearshore environment observed today. Atmospheric circulation and hydrodynamic models indicate that substantially weaker easterly trade winds and reduced significant wave height at 127 ka initiated robust reef development, which still persisted despite a dramatic increase in wave energy at 124 ka. By highlighting how variations in wave and wind regimes have shaped coral reef growth and resilience in the past, these findings underscore the value of integrating paleoecology and hydrodynamics to advance our understanding of reef stability under future climate change.

1 Introduction

Spanning approximately 129 to 116 thousand years before present, the Last Interglacial (LIG; Marine Isotope Stage 5e), has been widely used to reconstruct sea-level fluctuations (Kopp et al., 2009), temperature anomalies (Bova et al., 2021), and patterns of atmospheric and ocean circulation (Galaasen et al., 2014) under climate conditions slightly warmer than pre-industrial (Otto-Bliesner et al., 2013). These reconstructions provide critical constraints for sea-level rise and climate change models, ultimately informing projections of future changes (Edwards et al., 2021) and guiding policy decisions (Lee et al., 2023). Beyond refining estimates of LIG sea levels (Rovere et al., 2022) and tropical climate variability (Felis, 2020), the internal architecture and coral assemblages of fossil reefs can offer unique opportunities to reconstruct past ecological baselines (Pandolfi and Jackson, 2001) and infer paleo storms (Muhs and Simmons, 2017).

On the southern Caribbean islands of Aruba, Bonaire, and Curaçao (hereafter referred to as the ABC Islands), coral reef development is strongly influenced by prevailing winds and accompanying wave action. Along the southwest (leeward) coasts, fringing reefs persist, though they are in various stages of decline (Fig. A1a; (De Bakker et al., 2017)). In contrast, the windward (northeast) coasts are characterized by a Sargassum-covered, rocky submerged terrace that extends up to 150 m offshore and reaches depths of 12–15 m (Fig. A1b; (Focke, 1978)). Since the 1970s, when systematic observations began, this shallow windward zone has shown little to no significant reef growth above 12 meters water depth, aside from a few isolated patches (Van Duyl, 1985). On the windward side of the ABC islands, any existing reef growth is confined below approximately the 20-meter isobath, suggesting a persistent vertical limit to accretion (Fig. A1c).

Preserved on the ABC Islands as coral reef terraces located 5–10 m above present sea level, LIG reefs are occasionally incised by perennial streams creating gullies —locally called “*bocas*” on Aruba and “*bokas*” on Curaçao and Bonaire (hereafter referred to as “*bocas*”) — that expose complete fossil reef sequences (Alexander, 1961; Muhs et al., 2012). Notably, while modern windward reef development is virtually absent in shallow waters, fossil evidence shows that shallow-water reef crests and back-reef environments existed not only on the leeward sides—where modern reefs still occur—but also along the windward coasts during the LIG (Pandolfi et al., 1999).

The discrepancy between the distribution of modern and fossil reefs cannot be explained by human impacts. Although coral cover has declined across the Caribbean over the past 50 years, including the ABC Islands (Bak et al., 2005; Alvarez-Filip et al., 2009; De Bakker et al., 2017; Cramer et al., 2020), human development on all three islands has been concentrated primarily along the leeward coasts. Despite this, modern shallow-water reefs persist only on the leeward sides. In contrast, the undeveloped windward coasts lack any significant shallow reef development. This distribution pattern, coupled with less pronounced local anthropogenic pressure on the windward side, indicates that recent human activities are not responsible for the loss of reef development there. Furthermore, any global stressors (e.g., warming, acidification) would have affected both windward and leeward reefs alike, making the spatial asymmetry even more striking.

On geological timescales, reef development and accretion are primarily governed by accommodation space—the vertical space available for coral growth within the depositional environment—which fluctuates with sea-level changes over glacial-interglacial cycles (Camoin and Webster, 2015). Like their Last Interglacial counterparts, modern reefs have developed under conditions of rising relative sea level (RSL) since the Last Glacial Maximum (LGM). In the southern Caribbean, RSL rose at

rates of approximately 4 meters per thousand years around 8 ka (Khan et al., 2015), which is considerably slower than the estimated LIG glacial isostatic adjustment (GIA)-driven RSL rise of ~ 7.5 meters per thousand years around 128 ka (Dyer et al., 2021). This slower RSL rise during the LGM suggests that anticipated Holocene reef growth would reflect a keep-up morphology and is therefore insufficient to explain the absence of contemporary windward reef development. A missing mechanism must therefore exist that directly constrains reef accretion on the windward coasts of the ABC Islands.

Here, we test the hypothesis that the missing mechanism is linked to differences in wave conditions between the LIG and the present. To test this, we surveyed 17 LIG reef sites along the bocas on the windward coasts of the three ABC Islands (Fig. 1). At each site, we captured geospatially tagged and scaled digital twins of exposed reef outcrops, from which we extracted 153 paleoecological point intercept transects (PITs) across three chronostratigraphic stages of the LIG: Lower, Middle, and Upper. For each transect, we calculated mean hard coral cover (HC_A), relative genus-level coral cover (HC_G), and associated 95% confidence intervals (CIs) through bootstrapping. To evaluate spatial and temporal differences in HC_A , we fitted generalized linear mixed-effects (GLMER) models that accounted for site-specific variation. We also used a permutational multivariate analysis of variance (PERMANOVA) to test for shifts in HC_G across islands and LIG stages.

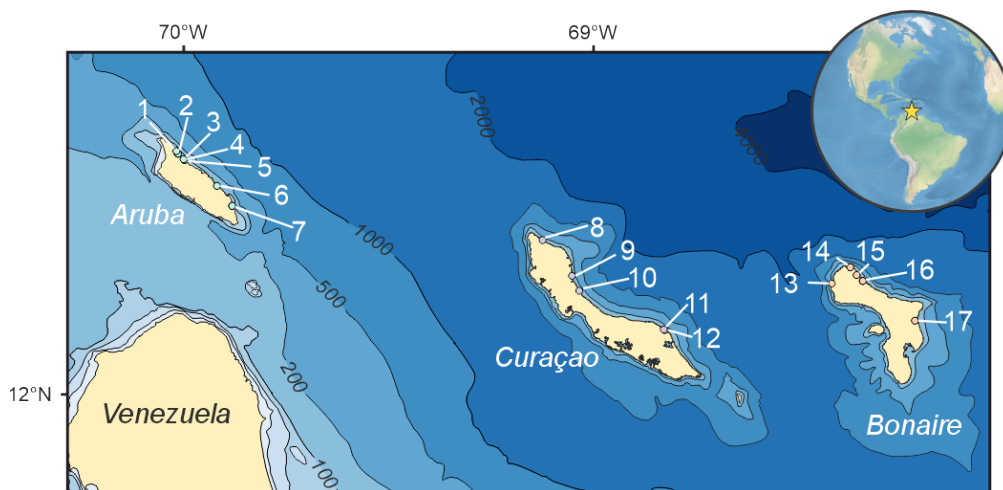


Figure 1. Map of ABC Islands with offshore depth contours. Sites for each island are as follows. Aruba: (1) Boca Urinama, (2) Boca Rancho Curason, (3) Boca Chikito, (4) Boca Blue Light, (5) boca 200 m southeast of Boca Chikito, (6) Dos Playa, (7) Rincon Beach. Curaçao: (8) Boka Kortalein, (9) Boka Patrick, (10) San Pedro, (11) Bock Labadera, (12) Boka Grandi. Bonaire: (13) Boka Slagbaai, (14) Boka Kokolishi, (15) Boka Chikitu, (16) Playa Grandi, (17) Boka Washikemba. Isobath, landmass, and basemap data are from Natural Earth.

To contextualize these ecological changes within broader climatic dynamics, we incorporated wind field outputs from global paleoclimate simulations as boundary conditions for local hydrodynamic models of the Caribbean Sea. These simulations allowed us to estimate average significant wave height, wave direction, and wave period at three key time slices: the onset of the LIG (127 ka), mid-LIG (124 ka), and the pre-industrial (PI) baseline. Our results show that, unlike today's windward coasts, the LIG reefs were characterized by well-developed structural complexity, which we attribute to reduced incident swell, itself a proxy for weakened easterly trade winds during the early stages of LIG sea-level rise. These findings not only shed light on the conditions that supported reef proliferation during past warm periods, but also offer insights into how future

changes in wind and wave regimes may influence the persistence and distribution of global reef systems under ongoing climate change.

2 Methods

2.1 Fossil reef surveys

We surveyed 17 sites where fossil reefs are exposed above sea level on the windward coasts of Aruba, Bonaire, and Curaçao (Fig. 1). In order to capture and analyze the entire exposed LIG reef sequence at each outcrop, land-based Structure from Motion/Multi-View Stereo (SfM/MVS) surveys were conducted. Using a 20.1 megapixel Sony DSC-RX100M3 camera (8.8 mm focal length and resolution of 5472 x 3648 pixels), around 750 photos were collected per outcrop. At least six ground control points (GCPs) were placed and measured using an Emlid Reach RS2+ dual-band dGNSS receiver (Rover) in each scene. On Curaçao, post-processing kinematic (PPK) positions were obtained from a second Emlid Reach RS2+ receiver recording a daily continuous static base station log from atop the CARMABI Research Station (12.122527°, -68.968600°). Similarly, on Bonaire, daily base station corrections were recorded by a second receiver affixed atop our accommodations (12.174713°, -69.289556°). The presence of a Continuously Operating Caribbean GPS Observational Network (COCONet; UNAVCO) site on Aruba (CN19) allowed us to process our rover data from Aruba against the published base station logs available through UNAVCO.

Post-processing of dGNSS data began by correcting the base data for Bonaire and Curaçao using the online Canadian Spatial Reference System Precise Point Positioning (CSRS-PPP) tool provided by Natural Resources Canada (NRCan). For reference, all CSRS-PPP outputs for each day are provided in the Electronic Supplementary Material SM-1. Using the corrected base position and elevation, rover survey logs were then post-processed using Emlid Studio Stop and Go (©Emlid Tech, v. 1.3). Resulting GCP positions were then converted from WGS84 ellipsoidal height to EGM08 (Pavlis et al., 2012) and the root-mean squares of all associated errors were calculated (see Electronic Supplementary Material Table SM-1). Next, digital twins of each site were created using the SfM/MVS software Agisoft Metashape Professional edition (version 2.1.0 build 17532), following a standard workflow for outcrop reconstruction (Boyden et al., 2022). Within each model, the above mentioned post-processed GCPs were then manually identified. Once constructed, high-resolution orthomosaics ($< 1.5 \text{ mm pix}^{-1}$) and quality reports were then exported and are available in the Electronic Supplementary Material SM-2.

In order to extract paleoecological from different parts of each outcrop captured via the digital twins, we subdivided each model into a maximum of three synchronously occurring reef subunits (Lower, Middle, and Upper). While time-averaging is of concern when drawing ecological data from fossil reefs (Frslich and Aberhan, 1990; Bernecker et al., 1999), we make a concerted effort to circumvent this by basing the subunits on relative elevation to the LIG coral reef terrace top as well as respective stratigraphic context. To further better constrain time-averaging and add replicability, three 10-m point intercept transects (PITs) were plotted horizontally with a vertical spacing of approximately 50 cm around the vertical midpoint of each subunit. At most sites, a total of nine PITs were selected per outcrop and, depending on outcrop dimensions and exposure, additional sets of PITs were collected at different sections of the outcrop and treated as additional sub-sites.

Several exposures we limited in vertical extent and therefore two or fewer subunits were surveyed. Drawing on the experience of previous paleo ecological surveys and as in-the-field time is not of issue, we utilize a PIT interval of 10 cm to achieve the most reliable ecological data (Greenstein et al., 1998; Pandolfi and Jackson, 2001; Ivkić et al., 2023). PIT data was extracted from the scaled orthomosaics in QGIS (v. 3.34.4-Prizren), where interval points were classified following a tiered scheme down to the genus level (Table A1). Care was taken to only classify in-growth position coral colonies as ‘live colonies’. Final site-specific, paleo benthic coverage was then calculated across each subunit by taking the average of classifications for each subunit (Lower, Middle, and Upper).

To assess the effect of stratigraphic age and island on the shift in HC_A , we fitted a Linear Mixed-Effects (LMM) model using the glmmTMB package in R (v. 4.4.3) (Brooks et al., 2017). The model included stratigraphic age and island as fixed effects and incorporated site as a random intercept to account for spatial variations across sites. None of the predictors included in the LMME were collinear with one another. Model validation diagnostics plots were obtained via the DHARMa package (Hartig, 2016) and indicate no significant issues (Fig. A4). Model residuals against fitted values showed homogeneity and no additional variance structure was added to the model (Fig. A5).

In order to compare the effect of stratigraphic age and island on changes in HC_G , we performed a PERMANOVA with 2000 permutations. In order to account for dominance of *Orbicella* spp. throughout the fossil, we first categorized all coral genera besides *A. palmata* and *Orbicella* spp. as *Other* and then applied a log-transformation to the data. Non-Metric Multidimensional Scaling (NMDS) ordination plots for all three islands across the three ages as well as for each island individually are shown in Figure A6a-d.

2.2 Paleo wave climate generation

To simulate the waves generated by winds under PI and LIG (127 ka, 124 ka) conditions, we extracted the annual average near-surface wind speed for these time periods from the comprehensive climate model time-slice simulations with CESM (Scussolini et al., (2023); LIG127 and PI) and the iCESM1.2 model (LIG124 and PI). The iCESM1.2 simulations have been carried out with the isotope-enabled Community Earth System Model, version 1.2 (for details on iCESM1.2, see Brady et al., (2019)) at a nominal 1° horizontal resolution in both the atmosphere and ocean components. For LIG124, greenhouse-gas concentrations follow Köhler et al. (2017), and orbital parameters have been prescribed according to Berger et al. (1993). Urban and crop land-cover types have been replaced in the LIG124 simulation by proportionally increasing the other plant-functional types in each gridbox of the land component. All other boundary conditions are identical to the PMIP4 pre-industrial setup (Otto-Bliesner et al., 2017)(see Electronic Supplementary Material SM-3 for LIG124 and PI model outputs). Sampling at a virtual buoy well offshore of the ABC Islands, we used resulting average wind speed and direction (LIG127 = 5.06 ms⁻¹: 320.08°, LIG124 = 9.71 ms⁻¹: 187.44°, PI= 10.58 ms⁻¹, 186.32°) to force wave generation over the southern Caribbean. In the hydrodynamic model, we activated the wind growth process (to create waves from the wind imposed at the boundaries) and used the white-capping formulation of Komen et al., (1984). This model was then run for 24 hours, in which the wind was kept constant over the entire modeling domain. Offshore significant wave heights and periods were taken from virtual buoys stationed in well before the deep-shallow wave transition for all scenarios. This negated any latent effect

varying paleo bathymetry and RSL may have had on incidental wave attributes. Hydrodynamic model set-up and outputs for the LIG127, LIG124 and PI scenarios are available in Electronic Supplementary Material SM-4.

3 Results and Discussion

3.1 Stratigraphic and Ecological Evolution of LIG Reefs on the ABC Islands

Our data show that hard coral cover on the ABC Islands remained relatively stable through the first two-thirds of the LIG. In stratigraphic terms, the Lower LIG corresponds to the earliest part of the interglacial, followed by the Middle and then the Upper LIG, which is the youngest and highest in the sequence. During the Lower LIG, HC_A was 40.3% (CI: 30.3–51.9%; Fig. 2), and it remained consistent in the Middle LIG at 42.3% (CI: 32.9–51.8%; $P > 0.1$; Fig. 2). However, a significant decline occurred in the Upper LIG, with HC_A dropping to 22.9% (CI: 15.6–30.0%; $P < 0.001$; Fig. 2). This temporal trend closely parallels the RSL trajectory derived from GIA models, as well as previously published sea-level indicators from Bonaire and Curaçao, which show that RSL plateaued after ~128 ka and remained relatively stable until the end of the LIG at ~116 ka (Fig. 3c; (Muhs et al., 2012; Rubio-Sandoval et al., 2021)).

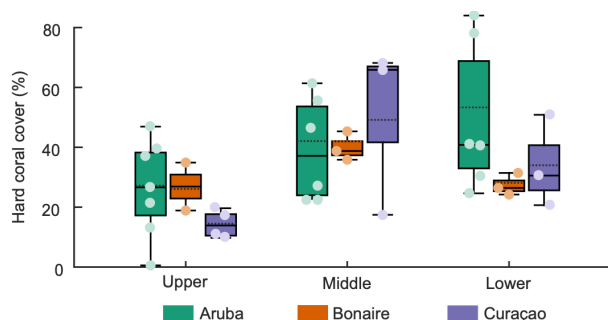


Figure 2. Island specific hard coral cover (HC_A) for each phase of the LIG coral growth. Boxplots show HC_A for each LIG growth phase for individual islands. The solid line within each boxplot marks the mean observed coral cover, while the dashed line represents predicted values from island-specific GLMER models.

Across the ABC Islands, the exposed facies of LIG fringing reefs generally represent shallow reef crest environments (Van Duyl, 1985) and are dominated by *Orbicella* spp. and *Acropora palmata*, with minor contributions from *Diploria* spp. and other locally abundant reef builders (Fig. 3a; (Pandolfi and Jackson, 2001)). Consistent with typical Quaternary reef sequences in the Caribbean (Greenstein et al., 1998), LIG reef development on the ABC Islands follows three successive phases: catch-up, keep-up, and lateral accretion (progradation) (Fig. 3b, (Woodroffe and Webster, 2014)).

During the first phase of the LIG, the initial sea-level transgression flooded the previously exposed Marine Isotope Stage 7 terrace (Muhs et al., 2012), allowing for the colonization of shallow substrates by *A. palmata* and *Orbicella* spp., and the development of a classic “catch-up” reef system. On Aruba, this phase is expressed as extensive hard coral cover during the Lower LIG ($HC_A = 49.9\%$, CI: 32.2–68.1%; Fig. 2), largely dominated by *Orbicella* spp. ($HC_G = 60.8\%$; Fig. 3). On

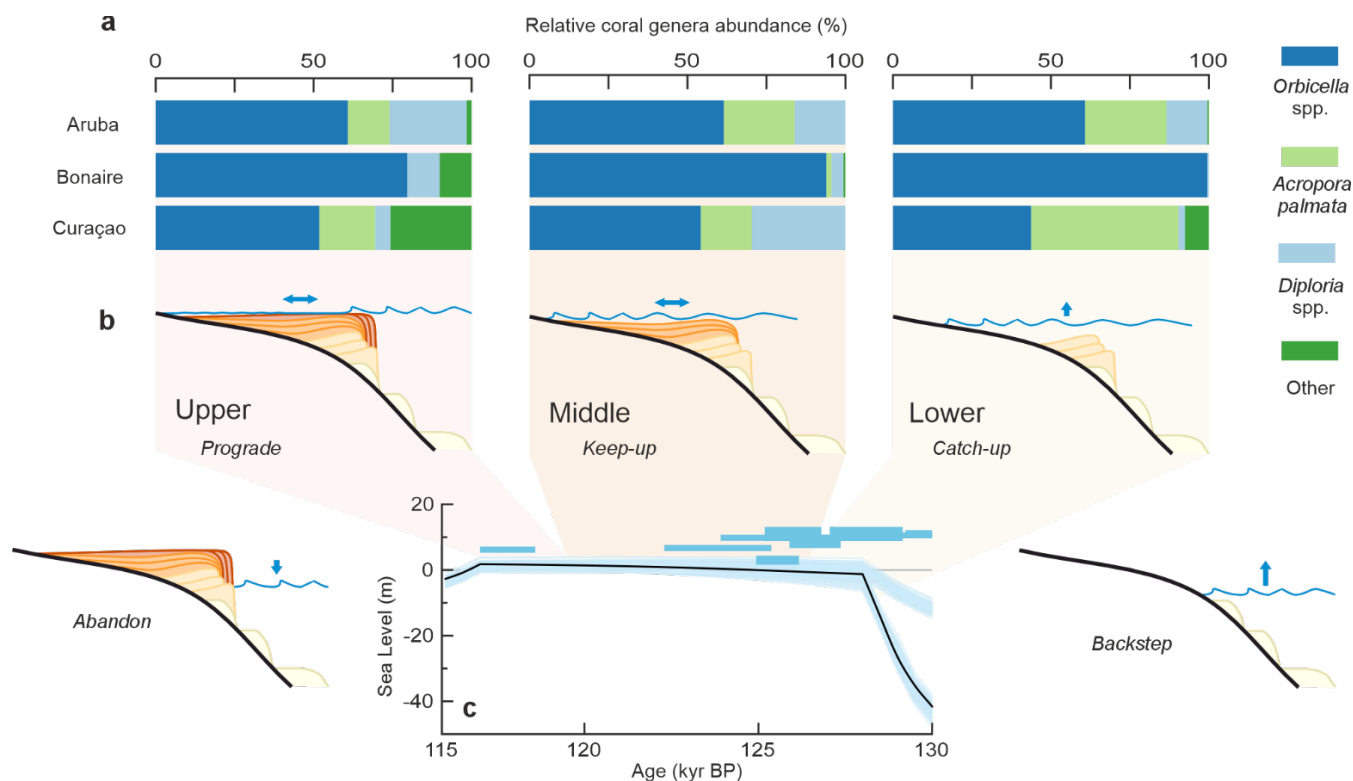


Figure 3. Coral cover, reef accretion history, and glacial isostatic adjustment–modeled sea levels during the LIG. (a) Hard coral cover at genera level (HCG) at each stratigraphic age and island. (b) Schematic of reef accretion through the LIG, with “Backstep” and “Abandon” phases inferred from the modeled glacial isostatic adjustment (GIA) curve. Shaded intervals indicate the approximate timing of the Lower, Middle, and Upper sequences relative to the GIA curve. The blue line and arrows show approximate sea level and its rate of change, respectively. Successive reef accretion phases are shaded in progressively darker tones to illustrate the build-up of the LIG reefal sequence. (c) GIA-modeled sea levels for Curaçao during the LIG, with the best-fit model from (Dyer et al., 2021) (black) and alternative model runs (light blue). Sea-level proxies from (Rubio-Sandoval et al., 2021) for the ABC Islands are shown with $\pm 2\sigma$ uncertainty boxes (light blue).

Curaçao, hard coral cover was lower overall ($HC_A = 34.1\%$, CI: 20.8–51.0%; Fig. 2), but the reef community included a greater proportion of *A. palmata* than on Aruba ($HC_G = 46.6\%$ vs. 25.8%, respectively; Fig. 3a). In contrast, Bonaire exhibited the lowest hard coral cover of the three islands during this interval ($HC_A = 27.5\%$, CI: 24.4–31.6%; Fig. 2) and was dominated almost entirely by *Orbicella* spp. (99.5%; Fig. 3a).

This early phase of reef growth coincided with a brief episode of cooler-than-modern sea surface temperatures ($\Delta SST = -2.1 \pm 0.7^\circ C$) around 126 ka (Brocas et al., 2016). The combination of temperature anomaly and increased seasonality during the early LIG (Brocas et al., 2019), may have led to cold-water stress events that suppressed reef development on the more oceanic setting of Bonaire and Curaçao (Lirman et al., 2011). Additionally, evidence for lower salinity during this period suggests enhanced runoff and turbidity, which could have further hindered coral growth (Brocas et al., 2019). However, given Aruba’s high coral cover at this time, the regionally uniform climate across the ABC Islands makes it unlikely that only two of the islands experienced significant differences in rainfall-driven turbidity (Alexander, 1961).

As the rate of RSL rise slowed after ~125 ka (Fig. 3c), reef development transitioned into a more stable “keep-up” regime. During this phase, the slow-growing but more resilient massive *Orbicella* spp. increasingly dominated the reef sequences (Fig. 3b, (Bruckner, 2003)). On Bonaire, coral cover significantly increased during this interval ($HC_A = 40.2\%$, CI: 36.0–45.5%; $P < 0.001$), and a similar trend was observed on Curaçao, where coral cover nearly doubled from 34.1% to 50.8% by the Middle LIG. However, due to substantial site-to-site variability on Curaçao, this increase was not statistically significant (CI = 17.6–68.3%, $P > 0.1$). In contrast, Aruba experienced a significant decrease in coral cover during the same period, dropping from 49.9% to 39.5% (CI = 27.6–52.2%, $P < 0.05$). This decline is likely not ecological in origin, but rather an artifact of exceptionally high initial coral cover during the catch-up phase, potentially driven by shallower antecedent bathymetry slopes and reef geometry on Aruba compared to the other two islands (Fig. 1; (Kleypas, 1997)). Despite the decline, coral cover on Aruba during the Middle LIG remained comparable to levels on Bonaire and Curaçao (Fig. 2). Notably, Middle LIG coral cover on the windward fossil reefs exceeded the peak cover values recorded on the leeward reefs of the ABC Islands when modern monitoring began in the 1970s (~45%; (Van Duyl, 1985)). This occurred under sea surface temperature and salinity conditions similar to those of the modern era (Felis et al., 2015), suggesting that these fossil reefs may have been more resilient to thermal stress than their contemporary counterparts.

Until the end of the LIG, RSL on Bonaire and Curaçao remained stable, with values constrained to 6.22 ± 0.95 m at 117.7 ± 0.8 ka (Obert et al., 2016) and 7.5 ± 1 m at 118.8 ka (Muhs et al., 2012), respectively (Fig. 3c). This sea-level stability is mirrored in a significant decline in coral cover on both Aruba and Curaçao between the Middle and Upper LIG, with reductions of 22.3% ($P < 0.001$) and 15.7% ($P < 0.02$), respectively (Fig. 2a). Both islands also exhibit a shift toward smaller, sub-massive colonies, including coral taxa such as *Diploria* spp. on Aruba and *Siderastrea* spp. and *Porites* spp. on Curaçao. However, significant changes in coral genus composition over time were observed only on Curaçao ($P < 0.05$). On Bonaire, coral cover also declined in the Upper LIG unit ($HC_A = 26.9\%$), but the decrease was not statistically significant ($P > 0.1$). This trend is likely the result of a reef crest migration further offshore and the local development of back-reef facies dominated by *Orbicella* spp. ($HC_G = 79.7\%$; Fig. 3a, (Pandolfi et al., 1999)). The transition to a progradational reef system coincided with a marked decrease in seasonality and a return of summer SSTs to near-modern levels (~27 °C), following the trajectory of summer insolation (Brocas et al., 2016).

Taken together, these results show that during the LIG, windward reef systems on the ABC Islands were ecologically robust and sustained high coral cover across multiple sea-level and temperature phases, with massive colonies (diameters > 2 m) of *Orbicella* spp. persisting until the closure of the LIG unit (Fig. A1). This stands in stark contrast to the present-day situation, where reef development is confined to the leeward coasts (Fig. A1a). Given that neither sea-level history nor local anthropogenic pressures can account for this spatial asymmetry, we next turn to the role of wind and wave climate. Specifically, we investigate whether differences in hydrodynamic forcing between the LIG and today can help explain the absence of shallow windward reefs in the modern setting.

3.2 Weaker trade winds and waves during the LIG

Changes in the intensity of the easterly trade winds across glacial–interglacial cycles have been widely documented using $\Delta\delta^{18}\text{O}$ proxies (Venancio et al., 2018). Climate model simulations for the LIG and PI periods show a marked decrease in wind speeds over the southern Caribbean at the onset of the LIG (~127 ka), with mean winds up to 4.5 m s^{-1} lower than PI values (Fig. 4a,c and Table A2; (Scussolini et al., 2023)). By mid-LIG (~124 ka), modeled mean wind speeds had increased substantially as compared to 127 ka, reaching up to 8.5 m s^{-1} in some areas (Fig. 4b). To translate these wind scenarios into wave conditions, we forced the 3D flow and wave model Delft3D (Deltares, ©2024) with respective constant wind fields for 24 model hours (Fig. 4a). The resulting wave simulations produced swells aligned with the prevailing trade-wind direction (Fig. 4a–c), but with substantially lower energy at the onset of the LIG (Fig. 4f). At 127 ka, the modeled average offshore significant wave height was just 0.3 m, rising to 0.9 m by 124 ka—a 253.5% increase within only 3 kyr (Fig. 4e,f). Despite this rise, wave heights at 124 ka remained 56.0% lower than under PI conditions and 75.9% lower than modern values (Fig. 4d and Fig. A2). Wave periods followed a similar trend, increasing from 2.1 to 3.9 seconds across the LIG. These values remained below both PI (5.1 s) and modern (7.0 s) averages, underscoring the reduced hydrodynamic energy of the LIG windward environment.

The fossil record has long been used to infer relative wave energy through the geomorphic context of reef outcrops (Geister, 1980). By combining this traditional approach with our modeled wave scenarios, we observe a clear imprint of a typical high-energy Caribbean reef (Macintyre, 1988), particularly through the contributions of *A. palmata* during initial reef development (Lower LIG) on both Aruba and Curaçao. Although *Orbicella* spp. dominates the fossil record, this likely reflects time-averaging across the first phase of reef accretion. Under stable conditions, the slower-growing *Orbicella* spp. can outcompete *A. palmata* over timescales of hundreds to thousands of years (Lirman, 2003). As reef frameworks thickened and prograded basinwards, the rising wave energy simulated for 124 ka was likely absorbed in part by the growing reef crest, creating favorable conditions for *Orbicella* spp. to continue dominating across all three islands (HCG: 54.2–94.0%).

Wave refraction and coastline orientation do influence significant wave heights around the ABC Islands, but this impact is relatively modest. For instance, modeled wave heights off Aruba’s windward coast are on average 23.6% lower than those off southeastern Bonaire across all modeled scenarios (Table A3). Yet, along Bonaire’s northwestern coast, specifically near Playa Grandi (Fig. 1), wave heights are nearly indistinguishable from those of Aruba (<1% difference), suggesting that localized island shadowing cannot fully account for differences in coral cover. Notably, the significant Middle LIG coral cover decline on Aruba ($\text{HCA} = 39.5\%$; Fig. 2) is better explained by the ~112% increase in wave height from Lower to Middle LIG, rather than spatial wave variation (~23.5% difference between Aruba and NW Curaçao at 124 ka). Furthermore, the lack of *A. palmata* on Bonaire likely reflects sampling bias: the LIG on Bonaire is predominantly sampled along the northwest coast—where predicted wave heights average 22% less than southeastern Bonaire across all three scenarios. Collectively, these observations indicate that temporal changes in wave energy were far more significant than spatial variations, underscoring that absolute wave climate—rather than local refraction—was the primary driver of reef structure during this interval.

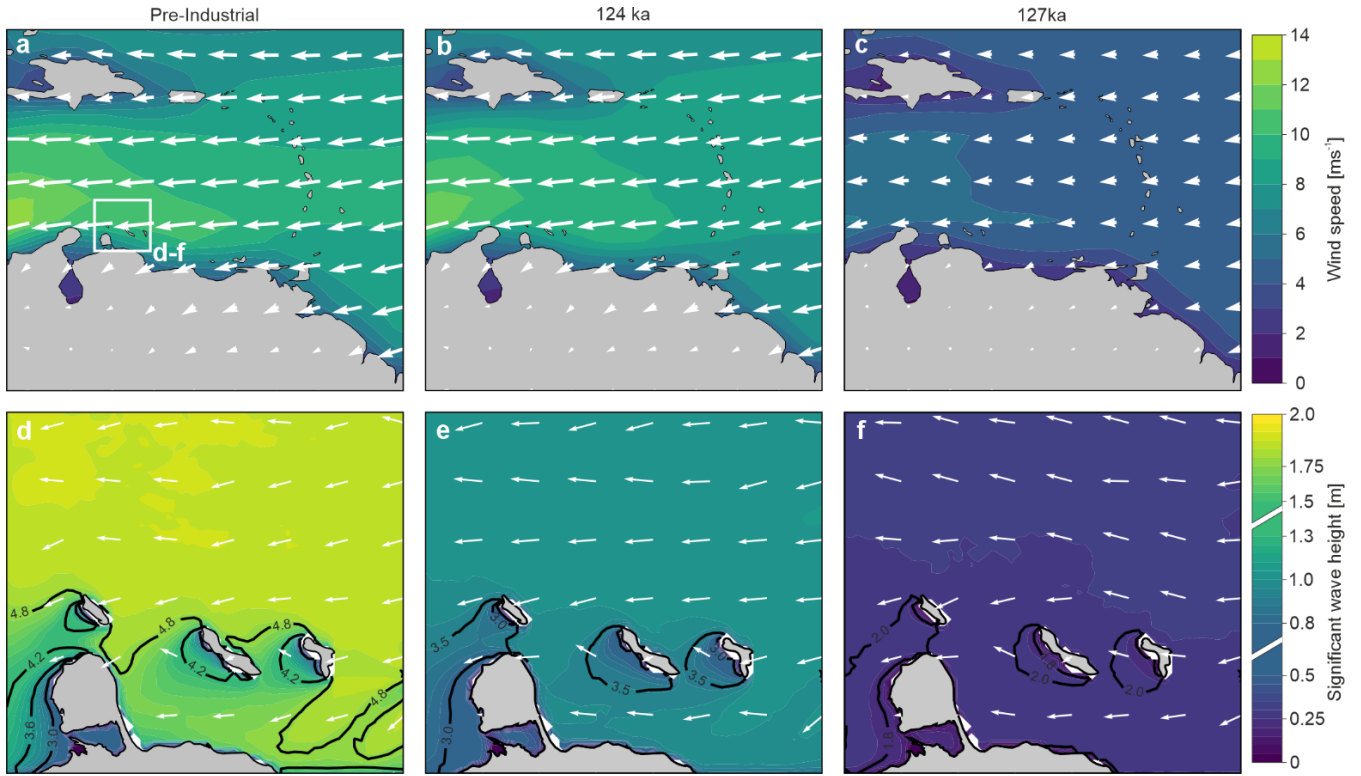


Figure 4. Modeled paleo wind and wave conditions in the southern Caribbean across the Pre-Industrial and LIG. Panels (a–c) show the modeled mean near-surface wind field (arrows) and wind speed (color) for (a) Pre-Industrial, (b) 124 ka, and (c) 127 ka. Panels (d–f) depict the modeled mean wave direction (arrows), wave period (contours), and significant wave height (color) for (d) Pre-Industrial, (e) 124 ka, and (f) 127 ka.

Although Holocene rates of relative sea-level rise were similar to those during the LIG (Pico, 2022), the resulting reef response diverged markedly. By ~ 3 ka BP, RSL had approached modern levels, and modest catch-up reef growth began. However, unlike in the LIG, where reduced wave energy allowed shallow reefs to establish, there is little evidence for extensive windward reef accretion during the Holocene. A distinct erosional notch at ~ 32 m water depth along Curaçao’s windward coast suggests the absence of subsequent Holocene reef build-up, as such growth would likely have obscured the feature. Instead, this submerged terrace system likely originated earlier, potentially during MIS 5c–a (Fig. A3; (Dyer et al., 2021; Malatesta et al., 2022)). Two main submerged terraces exist along the windward coasts of the ABC Islands: a shallower one between sea level and ~ 12 m depth, and a deeper one extending to ~ 40 m water depth. Both are significantly narrower than the LIG terrace, which reaches widths up to 700 m. The wider of the submerged terraces is less than 150 m across. While the submerged terraces lack chronological constraints, global sea-level estimates during MIS 5c–a range from -8 ± 6 m (Pico, 2022) to -22.3 m (Tawil-Morsink et al., 2022), with regional GIA-corrected RSL spanning approximately -20 m to -40 m (Fig. A3).

The remnants of the LIG terrace today represent only a fraction of the original reef’s lateral extent, due to post-depositional marine erosion (Malatesta et al., 2022). Based on global limestone cliff erosion rates (~ 29 m kyr $^{-1}$ from the GlobR2C2 database (Prémaillon et al., 2018)) and in situ measurements of coral reef erosion (~ 4.5 m kyr $^{-1}$; (Molina-Hernández et al.,

2022)), late Holocene and MIS 5c—a wave activity could have eroded up to 1.3 km of fossil reef structure. This erosion, combined with the virtual absence of modern windward shallow reef (Focke, 1978; Van Duyl, 1985), supports the idea that reef development attempted to restart in the early Holocene. Onshore deposits of large *A. palmata* rubble dating to $\sim 1044 \pm 905$ BP (Radtke et al., 2003) further hint at limited colonization. However, increasing wave energy through the pre-industrial and modern periods likely overwhelmed these nascent reef systems, preventing significant accretion and preserving the stark contrast between past and present reef distributions.

While the modern shallow windward reefs of the ABC islands are largely absent, windward reefs elsewhere in the Caribbean continue to persist despite ongoing anthropogenic pressures. Even if future warming is limited to 1.5 °C, the easterly trade winds in the southern Caribbean are projected to strengthen 0.2–0.4 ms⁻¹ relative to modern values, and a further 0.6 ms⁻¹ if warming exceeds 2.0 °C (Radtke et al., 2003). Although these increases are substantially lower than the differences in modeled wind velocity between PI and 127 ka (i.e., 5.52 ms⁻¹ for the ABC islands), they may nonetheless represent a tipping point for the stability of modern coral reefs. Enhanced wind speeds could increase significant wave heights along other windward Caribbean coasts, potentially applying hydrodynamic pressures beyond the resilience of these vulnerable ecosystems.

Conclusions

Our combined analysis of fossil reef ecology, hydrodynamic modeling, and coastal geomorphology reveals that reduced wind-driven wave energy during the early LIG created a narrow but critical window for reef initiation and persistence on the windward coasts of the ABC Islands. As sea level rose and wave energy increased, reefs transitioned into keep-up and progradational phases, maintaining substantial coral cover until the end of the LIG. In contrast, the Holocene—despite experiencing similar relative sea-level conditions—likely lacked a comparable drop in wave energy, and thus failed to support widespread shallow reef development on the windward coasts. Stronger trade winds during the late Holocene and modern periods, combined with long-term marine erosion, not only prevented new reef growth, but also erased much of the earlier reef structure.

This persistent spatial asymmetry in the existence of coral reefs—where fossil reefs flourished on both windward and leeward coasts during the LIG, but modern reefs are restricted to the leeward side—suggests that wave energy, rather than sea-level fluctuation or temperature alone, acts as the primary control on reef accretion at interstadial timescales. By quantifying shifts in coral cover and genus composition across stratigraphic phases of the LIG, we provide a novel paleoecological benchmark for validating wind and wave models. This integration of paleoecology and hydrodynamics offers a powerful new approach for understanding long-term reef stability. As global climate continues to warm, insights from the LIG can help predict how alterations in wind and wave patterns might critically affect coral reef stability and influence the spatial distribution of these ecosystems in the future.

Appendices

Table A1. Hierarchical benthic classifications used during the point-intercept transect surveys. Hard corals not in growth position were considered rubble, along with shell and other bioclastic debris. Other was used in the case of overgrowth or secondary deposition, covering the outcrop.

Level 1	Level 2	Level 3
Hard coral (HC)	Acropora	<i>Acropora cervicornis</i> <i>Acropora palmata</i> <i>Acropora prolifera</i>
	Branching	<i>Madracis</i> spp. <i>Porites</i> spp.
	Encrusting	<i>Agaricia</i> spp. <i>Colpophyllia</i> sp. <i>Dendrogyra</i> sp. <i>Diploria</i> spp. <i>Favia</i> sp. <i>Meandrina</i> spp. <i>Mussa</i> sp. <i>Orbicella</i> spp. <i>Porites</i> spp. <i>Siderastrea</i> spp.
	Tabular	<i>Cladocora</i> sp. <i>Eusmilia</i> sp.
	Massive	<i>Colpophyllia</i> sp. <i>Dichocoenia</i> sp. <i>Diploria</i> spp. <i>Isophyllia</i> spp. <i>Montastraea</i> sp. <i>Orbicella</i> spp. <i>Siderastrea</i> spp.
	Submassive	<i>Agaricia</i> spp. <i>Manicina</i> sp. <i>Meandrina</i> spp. <i>Orbicella</i> spp.
Algae (AG)		
Rock (RC)		
Rubble (RB)		
Sand (SD)		
Silt/clay (SI)		
Other (OT)		

Table A2. Annual average wind speed and direction at 10 meters altitude extracted from the Atmospheric circulation models of Scussolini et al., (2023) (LIG127) and the model described in this study (LIG124 and PI) at a virtual wind buoy.

BOUY_ ID	Latitude	Longitude	Wind speed (ms ⁻¹)			Direction (°)		
			127 ka	124 ka	PI	127 ka	124 ka	PI
Wind Buoy	12.831871	-67.373658	5.06	9.71	10.58	320.08	187.44	186.32

Table A3. Modeled significant wave heights and periods for each scenario (LIG127, LIG 124, and PI) at geographically important points along the windward side of the ABC Islands.

BOUY_ ID	Latitude	Longitude	Sig. wave height (m)			Period (s)		
			127 ka	124 ka	PI	127 ka	124 ka	PI
AUA	12.552197	-69.934555	0.23	0.82	1.43	2.20	4.07	5.45
NW-CUR	12.352197	-69.034554	0.29	1.04	1.73	2.08	3.70	4.82
SE-CUR	12.152197	-68.784554	0.27	0.94	1.55	2.04	3.51	4.52
NW-BON	12.302197	-68.334557	0.23	0.84	1.42	2.21	4.12	5.40
SE-BON	12.152197	-68.184555	0.30	1.05	1.78	2.14	3.91	5.08
Average			0.27	0.94	1.58	2.13	3.86	5.06

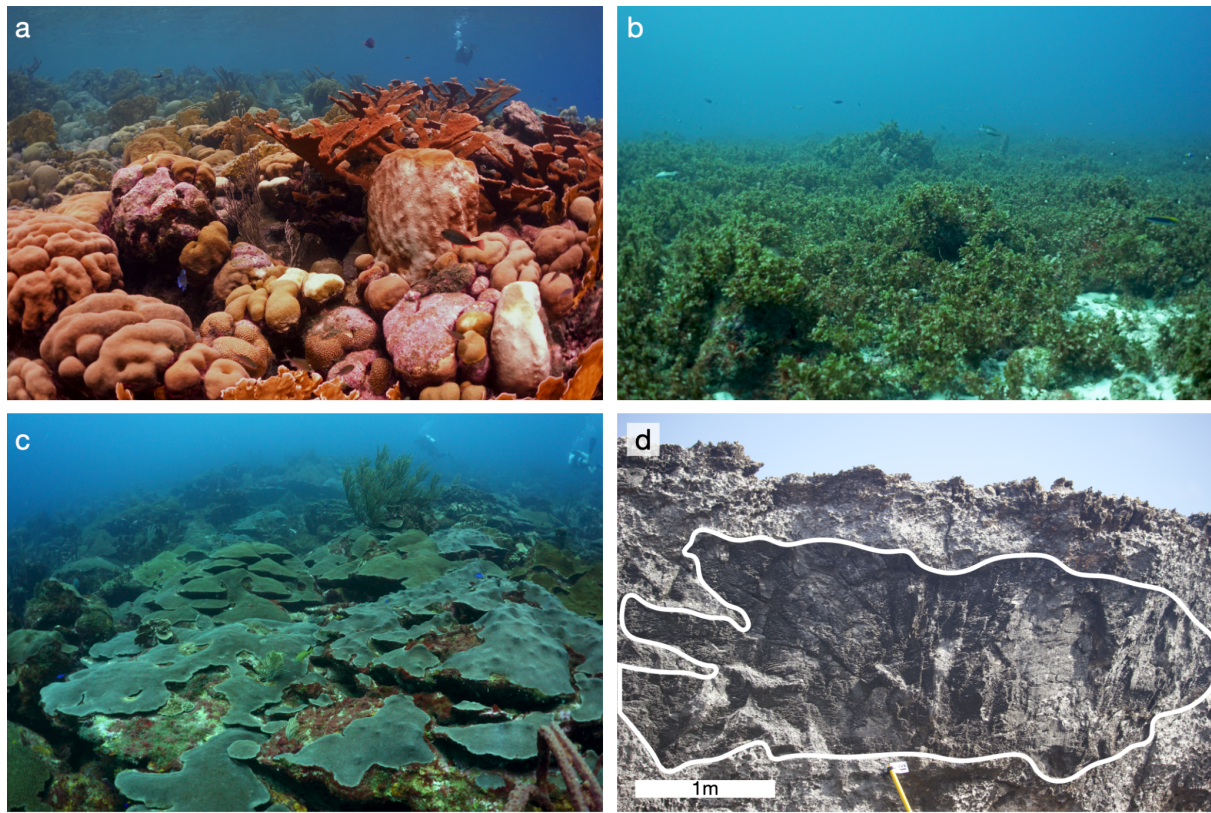


Figure A1. Asymmetry in hard coral distribution between the windward and leeward of the ABC Islands. (a) Representative *Acropora Palmata*, *Diploria* spp. and massive *Orbicella* spp. dominated shallow (<10 m water depth) fringing reef along the leeward coast of the ABC Islands. Photo taken at Rif Sint Marie, Curaçao - B. Mueller, 2020. (b) Sargassum-covered shallow submerged terrace, typical of the shallow (<10 m water depth) windward nearshore of the ABC islands. Photo taken at Boca Grandi, Curaçao - B. Mueller, 2016. (c) Encrusting to submassive *Orbicella* spp. dominated forereef slope, typical of deeper reef environments (>15 m water depth) to the windward of the ABC Islands. Photo taken at Boca Patrick, Curaçao - B. Mueller, 2016. (d) Massive *Orbicella* spp. in growth position near the top of the Last Interglacial section at BON-PlayaGrandi-T5F-McA, Playa Grandi, Bonaire - D. Chauveau, 2023.

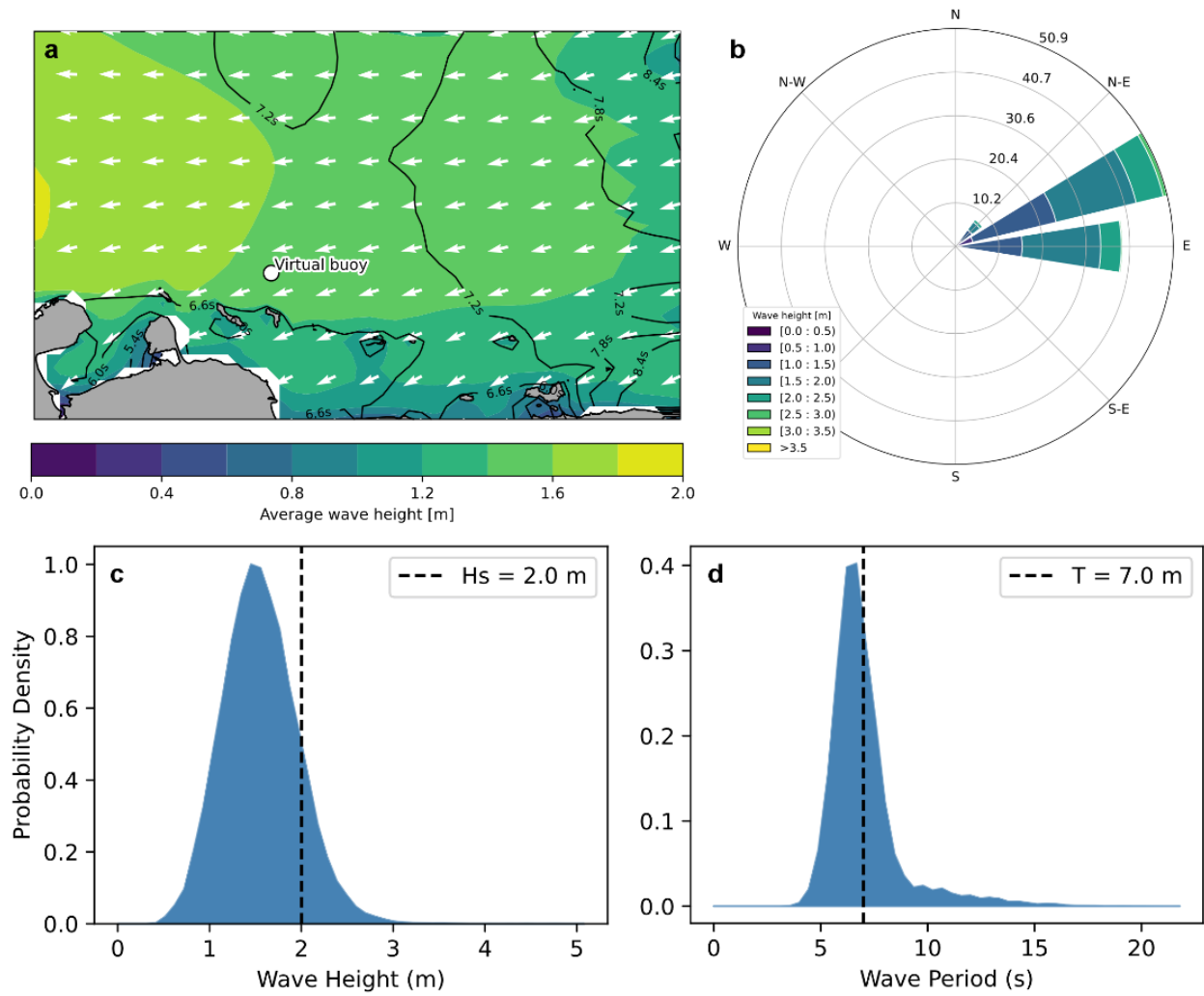


Figure A2. Modern wave conditions including (a) the average significant wave height, direction, and period from the Copernicus Marine Environment Monitoring Service (CMEMS) WAVEReanalysis (WAVERYS) (Law-Chune et al., 2021). WAVERYS oceanic currents from the GLORYS12 physical ocean reanalysis and assimilates wave heights from altimetry missions and (b) directional wave spectra from Sentinel 1 synthetic aperture radar from 2017 onwards. The dataset used in this figure includes data between 01 Jan 1980 and 31 Jan 2024. (c) Average significant wave height and (d) average period extracted from the virtual buoy indicated in Panel a.

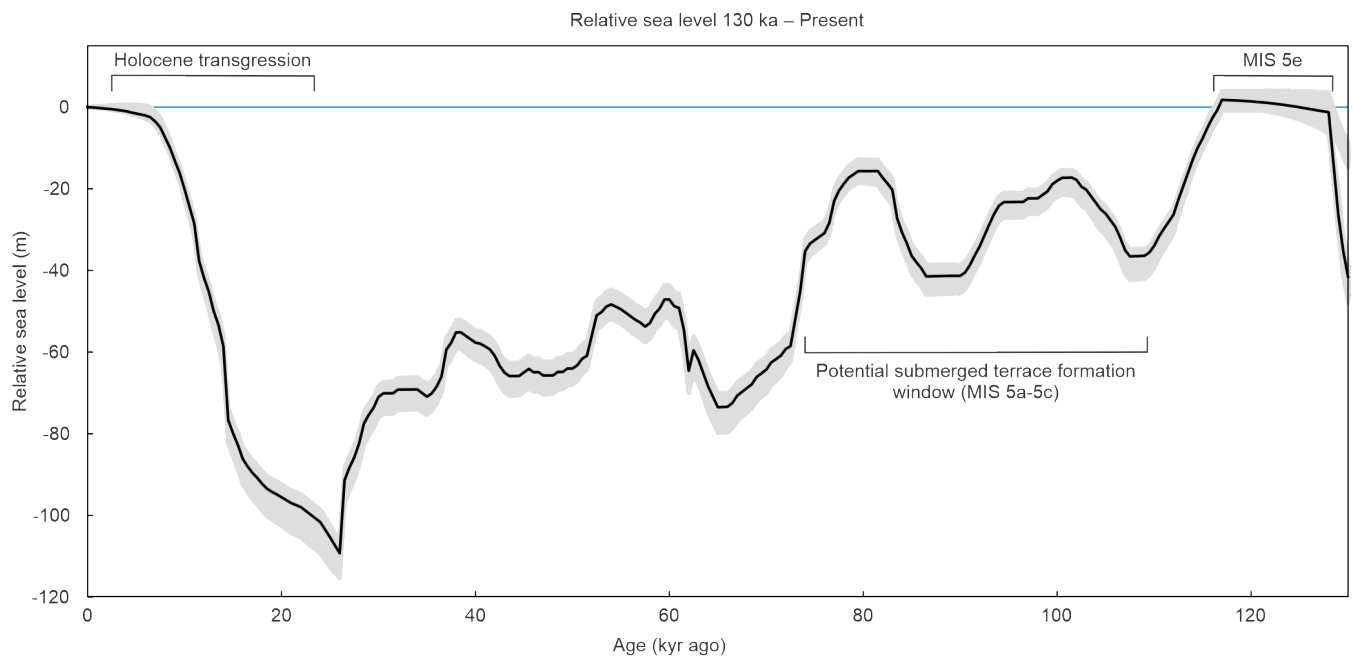


Figure A3: GIA predicted relative sea level from 130 ka to present from Dyer et al., (2021). Besides the Last Interglacial (MIS 5e), MIS 5a-c is also highlighted as a potential source of the submerged terrace at approximately 40 m below modern sea level.

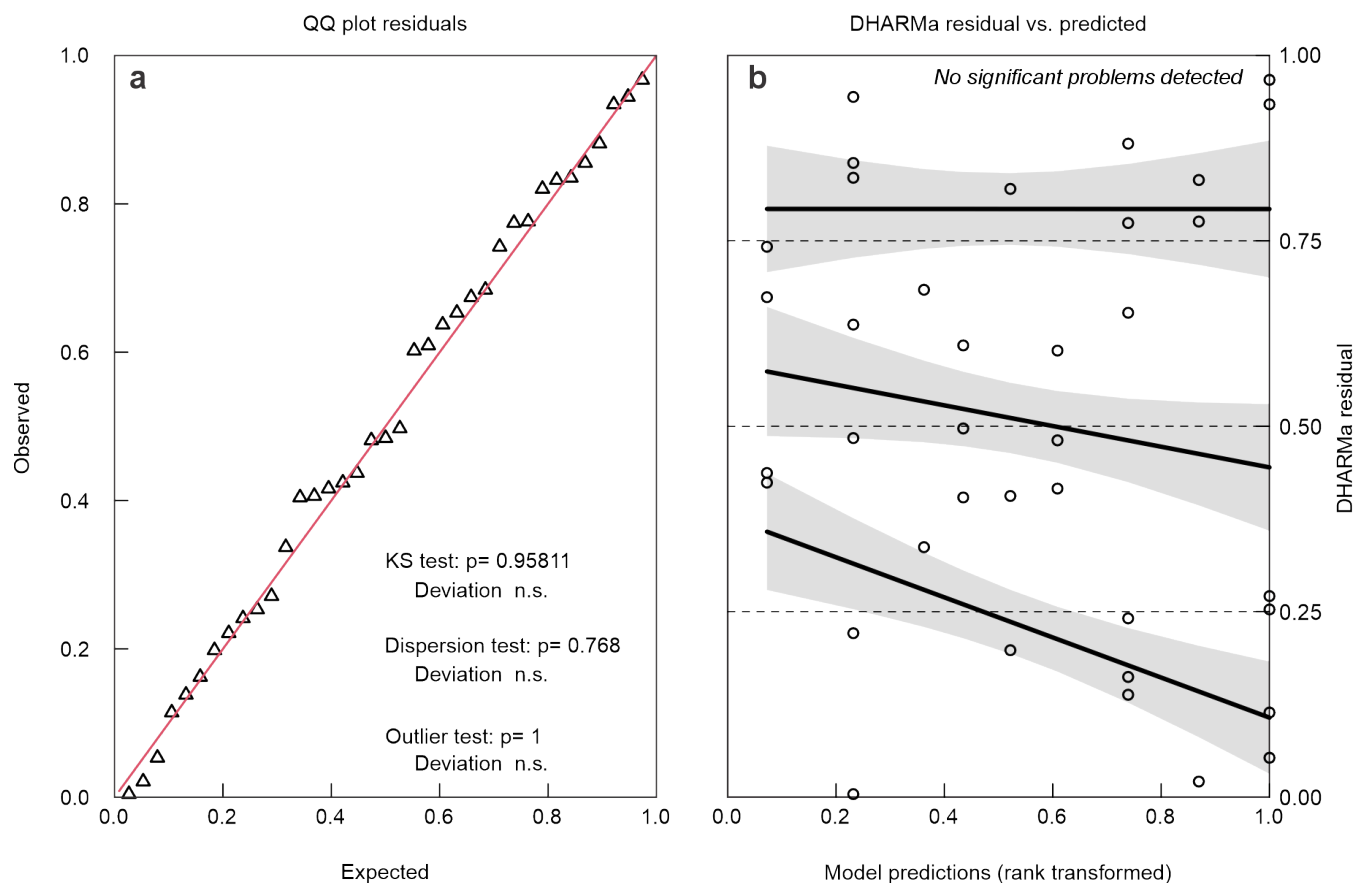


Figure A4: Results of DHARMA analysis (a) Q-Q residual plots, (b) DHARMA residual vs. predicted values.

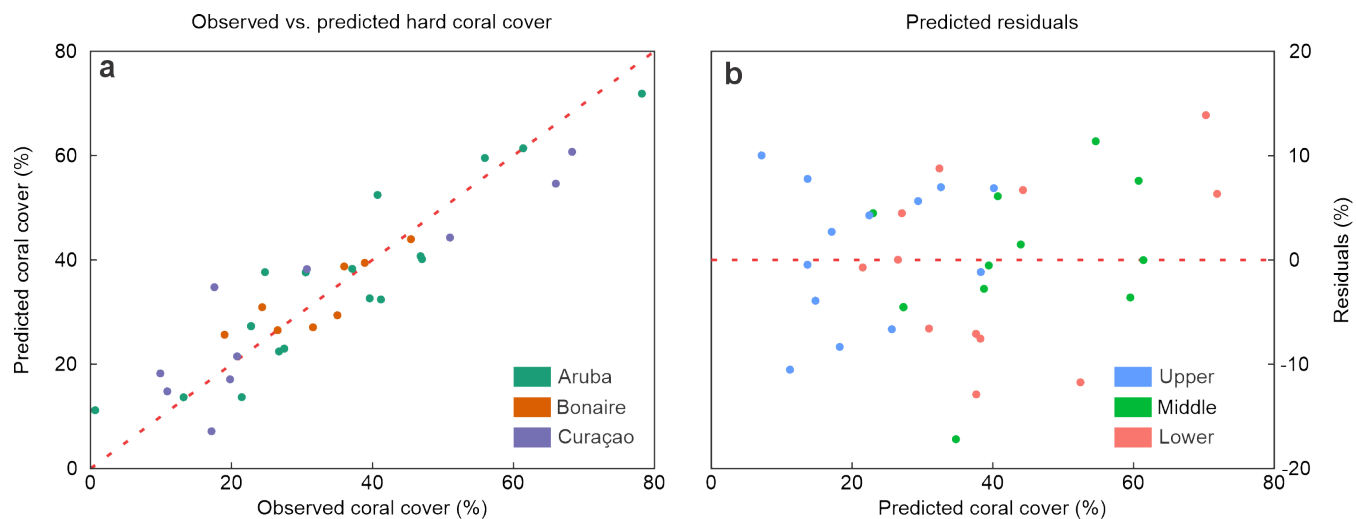


Figure A5: Resulting (a) observed versus predicted values and (b) plotted residuals from the LMME.

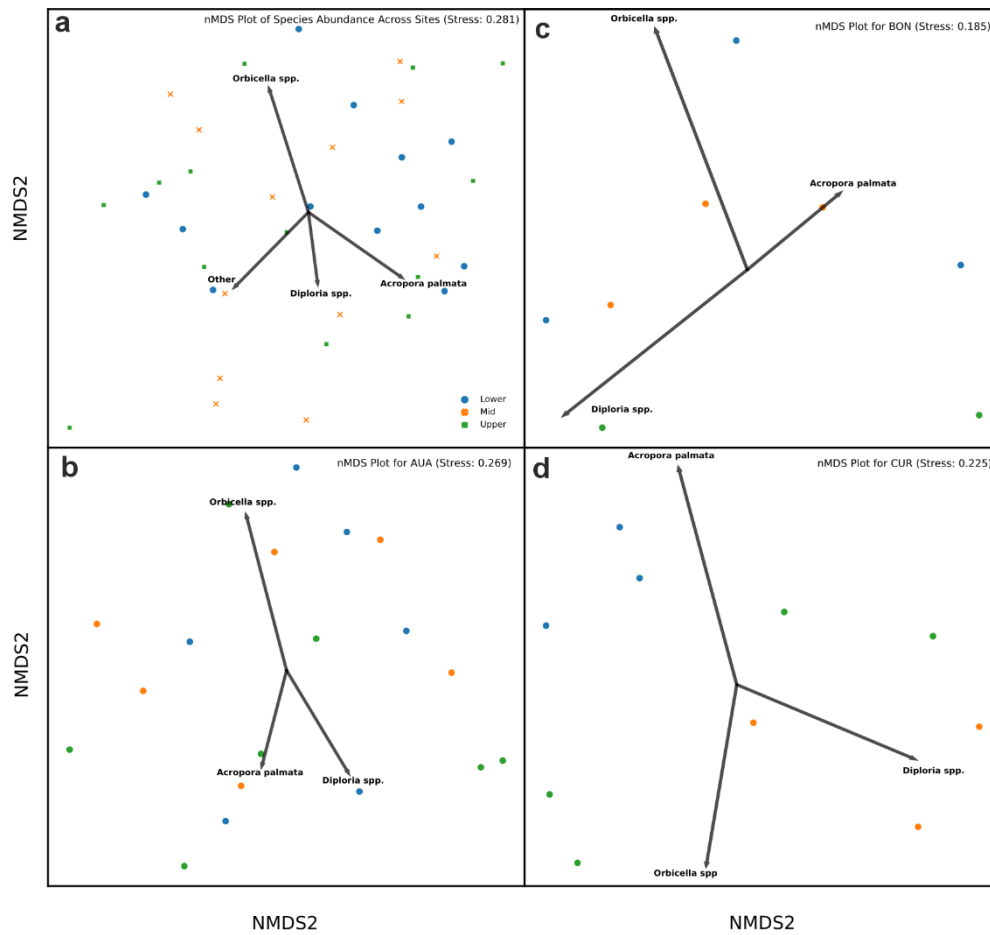


Figure A6: Ordination plots for (a) the whole ABC Island dataset, (b) Aruba, (c) Bonaire, and (d) Curaçao. Marker Colors and shapes relate to Lower (blue circles), Middle (orange crosses), and Upper (green squares).

Data availability

Electronic Supplementary Material is available in Zenodo with the identifier: [10.5281/zenodo.15674471](https://zenodo.org/record/15674471).

Author contribution

PB and AR conceived the idea, PB and AR wrote the manuscript. PB, AR, YCE, SB, GS, GS, DC, BM, PS, and MV took part in the survey of fossil sites. PB analyzed the fossil reef data with input by BM, CW, and SB. DL and UM set-up and ran the climate circulation model. AR and PB set-up and ran the hydrodynamic models. DL conducted the iCESM Earth-system model simulations with PI and 124 ka boundary conditions with guidance from UM. All authors have contributed to the text, revised it and agreed with its contents.

Conflict of interest

The authors declare that they have no conflict of interest.

Acknowledgements

The authors would like to acknowledge the fruitful discussions and support from Natasha Silva and Sietske van der Wal (Aruba Parke National, Aruba) and Roxanne Fransisca and Caren Eckrich (STINAPA, Bonaire). We would further like to acknowledge the computing resources granted to the project on the high-performance computers Lise and Emmy at the NHR Centers in Berlin and Göttingen jointly supported by the Federal Ministry of Research, Technology and Space (BMFTR) and the state governments participating in the National High-Performance Computing (NHR) joint funding program.

Funding

This project has received funding from the Deutsche Forschungsgemeinschaft (DFG, German Research Foundation), projects “Frozen in time: ecology of paleo reefs” (number 468589501, PB, SB, and CW) and “Tropical Atlantic-Pacific hydroclimate, variability and teleconnections during the Last Interglacial and the Holocene - Insights from earth-system modelling and corals (TAPIOLA)” (project number 468688677, DL and UM), both projects funded within the SPP 2299 “Tropical Climate Variability and Coral Reefs. A Past to Future Perspective on Current Rates of Change at Ultra-High Resolution” (project number 441832482). AR acknowledges funding from the European Research Council (ERC) under the European Union’s Horizon 2020 research and innovation programme (grant agreement no. 802414). DC would like to thank the ISblue project, Interdisciplinary graduate school for the blue planet (ANR-17-EURE-0015), co-funded by a grant from the French government under the program “Investissements d’Avenir” embedded in France 2030. DL and UM gratefully acknowledge the computing resources granted to them on the high-performance computers Lise and Emmy at the NHR Centers in Berlin and Göttingen jointly supported by the Federal Ministry of Research, Technology and Space (BMFTR) and the state governments participating in the National High-Performance Computing (NHR) joint funding program (<http://www.nhr-verein.de/en/our-partners>).

References

- Alexander, C. S.: The marine terraces of Aruba, Bonaire, and Curaçao, Netherlands Antilles, *Annals of the Association of American Geographers*, 51, 102--123, 1961.
- Alvarez-Filip, L., Dulvy, N. K., Gill, J. A., and Côté: Flattening of Caribbean coral reefs: region-wide declines in architectural complexity, *Proceedings of the Royal Society B: Biological Sciences*, 276, 3019--3025, 10.1098/rspb.2009.0339, 2009.
- Bak, R. P. M., Nieuwland, G., and Meesters, E. H.: Coral reef crisis in deep and shallow reefs: 30 years of constancy and change in reefs of Curaçao and Bonaire, *Coral reefs*, 24, 475--479, 10.1007/s00338-005-0009-1, 2005.

Berger, A., Loutre, M. F., and Tricot, C.: Insolation and Earth's orbital periods, *Journal of Geophysical Research: Atmospheres*, 98, 10341-10362, 10.1029/93JD00222, 1993.

Bernecker, M., Weidlich, O., and Flgel, E.: Response of Triassic reef coral communities to sea-level fluctuations, storms and sedimentation: evidence from a spectacular outcrop (Adnet, Austria), *Facies*, 40, 229--279, 10.1007/BF02537476, 1999.

Bova, S., Rosenthal, Y., Liu, Z., Godad, S. P., and Yan, M.: Seasonal origin of the thermal maxima at the Holocene and the last interglacial, *Nature*, 589, 548-553, 10.1038/s41586-020-03155-x, 2021.

Boyden, P., Weil-Accardo, J., Deschamps, P., Godeau, N., Jaosedy, N., Guihou, A., Rajaonarivelo, M. N., O'Leary, M., Humblet, M., and Rovere, A.: Revisiting Battistini: Pleistocene Coastal Evolution of Southwestern Madagascar, *OpenQuaternary*, 10.5334/oq.112, 2022.

Brady, E., Stevenson, S., Bailey, D., Liu, Z., Noone, D., Nusbaumer, J., Otto-Bliesner, B. L., Tabor, C., Tomas, R., and Wong, T.: The connected isotopic water cycle in the Community Earth System Model version 1, *Journal of Advances in Modeling Earth Systems*, 11, 2547-2566, 10.1029/2019MS001663, 2019.

Brocas, W. M., Felis, T., and Mudsee, M.: Tropical Atlantic cooling and freshening in the middle of the last interglacial from coral proxy records, *Geophysical Research Letters*, 46, 8289--8299, 10.1029/2019GL083094, 2019.

Brocas, W. M., Felis, T., Obert, J. C., Gierz, P., Lohmann, G., Scholz, D., Killing, M., and Scheffers, S. R.: Last interglacial temperature seasonality reconstructed from tropical Atlantic corals, *Earth and Planetary Science Letters*, 449, 418--429, 10.1016/j.epsl.2016.06.005, 2016.

Brooks, M. E., Kristensen, K., Van Benthem, K. J., Magnusson, A., Berg, C. W., Nielsen, A., Skaug, H. J., Mächler, M., and Bolker, B. M.: glmmTMB balances speed and flexibility among packages for zero-inflated generalized linear mixed modeling, 2017.

Bruckner, A. W.: *Acropora palmata*, *Acropora Workshop: Potential Application of the US Endangered Species Act as a Conservation Strategy* 2003.

Camoin, G. F. and Webster, J. M.: Coral reef response to Quaternary sea-level and environmental changes: State of the science, *Sedimentology*, 62, 401-428, ISSN = 0037-0746, 10.1111/sed.12184, 2015.

Cramer, K., Jackson, J. B. C., Donovan, M. K., Greenstein, B. J., Korpanty, C. A., Cook, G. M., and Pandolfi, J. M.: Widespread loss of Caribbean acroporid corals was underway before coral bleaching and disease outbreaks, *Science Advances*, 6, eaax9395, 10.1126/sciadv.aax9395, 2020.

De Bakker, D. M., Van Duyl, F. C., Bak, R. P. M., Nugues, M. M., Nieuwland, G., and Meesters, E. H.: 40 Years of benthic community change on the Caribbean reefs of Curaçao and Bonaire: the rise of slimy cyanobacterial mats, *Coral Reefs*, 36, 355--367, 10.1007/s00338-016-1534-9, 2017.

Dyer, B., Austermann, J., D'Andrea, W. J., Creel, R. C., Sandstrom, M. R., Cashman, M., Rovere, A., and Raymo, M. E.: Sea-level trends across The Bahamas constrain peak last interglacial ice melt, *Proceedings of the National Academy of Sciences*, 118, e2026839118, 10.1073/pnas.2026839118, 2021.

Edwards, T. L., Nowicki, S., Marzeion, B., Hock, R., Goelzer, H., Seroussi, H., Jourdain, N. C., Slater, D. A., Turner, F. E., and Smith, C. J.: Projected land ice contributions to twenty-first-century sea level rise, *Nature*, 593, 74-82, 10.1038/s41586-021-03302-y, 2021.

- Felis, T.: Extending the instrumental record of ocean-atmosphere variability into the last interglacial using tropical corals, *Oceanography*, 33, 68--79, 10.5670/oceanog.2020.209, 2020.
- Felis, T., Giry, C., Scholz, D., Lohmann, G., Pfeiffer, M., Ptzold, J., Klling, M., and Scheffers, S. R.: Tropical Atlantic temperature seasonality at the end of the last interglacial, *Nature Communications*, 6, 6159, 10.1038/ncomms7159, 2015.
- Focke, J. W.: Subsea (0-40 m) terraces and benches, windward off Curaçao, Netherlands Antilles, *Leidse Geologische Mededelingen*, 51, 95--102, 1978.
- Frslich, F. T. and Aberhan, M.: Significance of time-averaging for palaeocommunity analysis, *Lethaia*, 23, 143--152, 10.1111/j.1502-3931.1990.tb01355.x, 1990.
- Galaasen, E., Ninnemann, U., Nil, I., Kleiven, H. F., Rosenthal, Y., Kissel, C., and Hodell, D.: Rapid Reductions in North Atlantic Deep Water During the Peak of the Last Interglacial Period, *Science*, 343, 1129 - 1132, 10.1126/science.1248667, 2014.
- Geister, J.: Calm-water reefs and rough-water reefs of the Caribbean Pleistocene, *Acta Palaeontologica Polonica*, 25, 1980.
- Greenstein, B. J., Curran, H. A., and Pandolfi, J. M.: Shifting ecological baselines and the demise of *Acropora cervicornis* in the western North Atlantic and Caribbean Province: a Pleistocene perspective, *Coral Reefs*, 17, 249--261, 10.1007/s003380050125, 1998.
- Hartig, F.: DHARMA: residual diagnostics for hierarchical (multi-level/mixed) regression models, CRAN: Contributed Packages, 2016.
- Ivkić, A., Puff, F., Kroh, A., Mansour, A., Osman, M., Hassan, M., Ahmed, A. E. H., and Zuschin, M.: Three common sampling techniques in Pleistocene coral reefs of the Red Sea: a comparison, *Geological Society, London, Special Publications*, 529, 223-242, 10.1144/SP529-2022-227, 2023.
- Khan, N., Erica, L. A., Shaw, T., Vacchi, M., Walker, J., Peltier, W., Robert, E. K., Horton, B., and Horton, B.: Holocene Relative Sea-Level Changes from Near-, Intermediate-, and Far-Field Locations, *Current Climate Change Reports*, 1, 247-262, 10.1007/s40641-015-0029-z, 2015.
- Kleypas, J. A.: Modeled estimates of global reef habitat and carbonate production since the last glacial maximum, *Paleoceanography*, 12, 533--545, 10.1029/97PA01134, 1997.
- Köhler, P., Nehrbass-Ahles, C., Schmitt, J., Stocker, T. F., and Fischer, H.: A 156 kyr smoothed history of the atmospheric greenhouse gases CO₂, CH₄, and N₂O and their radiative forcing, *Earth System Science Data*, 9, 363-387, 10.5194/essd-9-363-2017, 2017.
- Komen, G. J., Hasselmann, S., and Hasselmann, K.: On the existence of a fully developed wind-sea spectrum, *Journal of physical oceanography*, 14, 1271--1285, 10.1175/1520-0485(1984)014<1271:OTEOAF>2.0.CO;2, 1984.
- Kopp, R. E., Simons, F. J., Mitrovica, J. X., Maloof, A. C., and Oppenheimer, M.: Probabilistic assessment of sea level during the last interglacial stage, *Nature*, 462, 863-867, 10.1038/nature08686, 2009.
- Lee, H., Calvin, K., Dasgupta, D., Krinner, G., Mukherji, A., Thorne, P., Trisos, C., Romero, J., Aldunce, P., Barret, K., and et al.: IPCC, 2023: Climate Change 2023: Synthesis Report, Summary for Policymakers. Contribution of Working Groups I, II and III to the Sixth Assessment Report of the Intergovernmental Panel on Climate Change Core Writing Team, H. Lee and J. Romero (eds.) . IPCC, Geneva, Switzerland., 10.59327/IPCC/AR6-9789291691647.001, 2023.

Lirman, D.: A simulation model of the population dynamics of the branching coral *Acropora palmata* Effects of storm intensity and frequency, *Ecological modelling*, 161, 169--182, 10.1016/S0304-3800(02)00346-0, 2003.

Lirman, D., Schopmeyer, S., Manzello, D., Gramer, L. J., Precht, W. F., Muller-Karger, F., Banks, K., Barnes, B., Bartels, E., Bourque, A., and et al.: Severe 2010 cold-water event caused unprecedented mortality to corals of the Florida reef tract and reversed previous survivorship patterns, *PLoS one*, 6, e23047, 10.1371/journal.pone.0023047, 2011.

Macintyre, I. G.: Modern coral reefs of western Atlantic: new geological perspective, *AAPG bulletin*, 72, 1360--1369, 10.1306/703C99A1-1707-11D7-8645000102C1865D, 1988.

Malatesta, L. C., Finnegan, N. J., Huppert, K. L., and Carreo, E. I.: The influence of rock uplift rate on the formation and preservation of individual marine terraces during multiple sea-level stands, *Geology*, 50, 101--105, 10.1130/G49245.1, 2022.

Molina-Hernández, A., Medellín-Maldonado, F., Lange, I. D., Perry, C. T., and Álvarez-Filip, L.: Coral reef erosion: In situ measurement on different dead coral substrates on a Caribbean reef, *Limnology and Oceanography*, 67, 2734-2749, 10.1002/lno.12234, 2022.

Muhs, D. R. and Simmons, K. R.: Taphonomic problems in reconstructing sea-level history from the late Quaternary marine terraces of Barbados, *Quaternary Research*, 88, 409-429, 10.1017/qua.2017.70, 2017.

Muhs, D. R., Pandolfi, J. M., Simmons, K. R., and Schumann, R. R.: Sea-level history of past interglacial periods from uranium-series dating of corals, Curaçao, Leeward Antilles islands, *Quaternary Research*, 78, 157--169, 10.1016/j.yqres.2012.05.008, 2012.

Obert, J. C., Scholz, D., Felis, T., Brocas, W. M., Jochum, K. P., and Andreae, M. O.: ²³⁰Th/U dating of Last Interglacial brain corals from Bonaire (southern Caribbean) using bulk and theca wall material, *Geochimica et Cosmochimica Acta*, 178, 20--40, 10.1016/j.gca.2016.01.011, 2016.

Otto-Bliesner, B. L., Rosenbloom, N., Stone, E. J., McKay, N. P., Lunt, D. J., Brady, E. C., and Overpeck, J. T.: How warm was the last interglacial? New model--data comparisons, *Philosophical Transactions of the Royal Society A: Mathematical, Physical and Engineering Sciences*, 371, 20130097, 10.1098/rsta.2013.0097, 2013.

Otto-Bliesner, B. L., Braconnot, P., Harrison, S. P., Lunt, D. J., Abe-Ouchi, A., Albani, S., Bartlein, P. J., Capron, E., Carlson, A. E., and Dutton, A.: The PMIP4 contribution to CMIP6--Part 2: Two interglacials, scientific objective and experimental design for Holocene and Last Interglacial simulations, *Geoscientific Model Development*, 10, 3979-4003, 10.5194/gmd-10-3979-2017, 2017.

Pandolfi, J. M. and Jackson, J. B. C.: Community structure of Pleistocene coral reefs of Curaçao, Netherlands Antilles, *Ecological monographs*, 71, 49--67, 10.1890/0012-9615(2001)071[0049:CSOPCR]2.0.CO;2, 2001.

Pandolfi, J. M., Llewellyn, G., and Jackson, J. B. C.: Pleistocene reef environments, constituent grains, and coral community structure: Curaçao, Netherlands Antilles, *Coral Reefs*, 18, 107--122, 10.1007/s003380050165, 1999.

Pavlis, N. K., Holmes, S. A., Kenyon, S. C., and Factor, J. K.: The development and evaluation of the Earth Gravitational Model 2008 (EGM2008), *Journal of geophysical research: solid earth*, 117, 2012.

Pico, T.: Toward new and independent constraints on global mean sea-level highstands during the Last Glaciation (Marine Isotope Stage 3, 5a, and 5c), *Paleoceanography and Paleoclimatology*, 37, e2022PA004560, 10.1029/2022PA004560, 2022.

Prémaillon, M., Regard, V., Dewez, T. J., and Auda, Y.: GlobR2C2 (Global Recession Rates of Coastal Cliffs): a global relational database to investigate coastal rocky cliff erosion rate variations, *Earth Surface Dynamics*, 6, 651-668, 10.5194/esurf-6-651-2018, 2018.

Radtke, U., Schellmann, G., Scheffers, A., Kelletat, D., Kromer, B., and Kasper, H. U.: Electron spin resonance and radiocarbon dating of coral deposited by Holocene tsunami events on Curaçao, Bonaire and Aruba (Netherlands Antilles), *Quaternary Science Reviews*, 22, 1309--1315, 10.1016/S0277-3791(03)00036-2, 2003.

Rovere, A., Ryan, D. D., Vacchi, M., Dutton, A., Simms, A. R., and Murray-Wallace, C. V.: The world atlas of last interglacial shorelines (version 1.0), *Earth System Science Data Discussions*, 2022, 1--37, 10.5194/essd-15-1-2023, 2022.

Rubio-Sandoval, K., Rovere, A., Cerrone, C., Stocchi, P., Lorscheid, T., Felis, T., Petersen, A.-K., and Ryan, D. D.: A review of last interglacial sea-level proxies in the western Atlantic and southwestern Caribbean, from Brazil to Honduras, *Earth System Science Data*, 13, 4819--4845, 10.5194/essd-13-4819-2021, 2021.

Scussolini, P., Dullaart, J., Muis, S., Rovere, A., Bakker, P., Coumou, D., Renssen, H., Ward, P. J., and Aerts, J. C. J. H.: Modeled storm surge changes in a warmer world: the Last Interglacial, *Climate of the Past*, 19, 141--157, 10.5194/cp-19-141-2023, 2023.

Tawil-Morsink, K., Austermann, J., Dyer, B., Dumitru, O. A., Precht, W. F., Cashman, M., Goldstein, S. L., and Raymo, M. E.: Probabilistic investigation of global mean sea level during MIS 5a based on observations from Cave Hill, Barbados, *Quaternary Science Reviews*, 295, 107783, 10.1016/j.quascirev.2022.107783, 2022.

Van Duyl, F. C.: Atlas of the Living Reefs of Curaçao and Bonaire (Netherlands Antilles), Foundation for Scientific Research in Surinam and the Netherlands Antilles, 117, 1985.

Venancio, I. M., Mulitza, S., Govin, A., Santos, T. P., Lessa, D. O., Albuquerque, A. L. S., Chiessi, C. M., Tiedemann, R., Vahlenkamp, M., Bickert, T., and et al.: Millennial-to orbital-scale responses of western equatorial Atlantic thermocline depth to changes in the trade wind system since the last interglacial, *Paleoceanography and Paleoclimatology*, 33, 1490--1507, 10.1029/2018PA003437, 2018.

Woodroffe, C. D. and Webster, J. M.: Coral reefs and sea-level change, *Marine Geology*, 352, 248--267, 10.1016/j.margeo.2013.12.006, 2014.